Working Paper 2016:2

Department of Economics
School of Economics and Management

Cross-Commodity News Transmission and Volatility Spillovers in the German Energy Markets

Rikard Green
Karl Larsson
Veronika Lunina
Birger Nilsson

January 2016
Revised: October 2017

LUND
UNIVERSITY

Cross-Commodity News Transmission and Volatility Spillovers in the German Energy Markets

Rikard Green[a], Karl Larsson[b], Veronika Lunina[c,*], Birger Nilsson[c]

[a] *E.ON Sverige AB, S-20509 Malmö, Sweden*
[b] *Statistics Sweden, S-70189 Örebro, Sweden*
[c] *Knut Wicksell Centre for Financial Studies and Department of Economics, School of Economics and Management, Lund University, S-22007 Lund, Sweden*

Abstract

This study investigates volatility spillovers to electric power from large exogenous shocks in the prices of gas, coal, and carbon emission allowances in the German energy market. Our sample ranges from 2008 to 2016 and covers periods of different market conditions. We use a general VAR-BEKK model and the volatility impulse response function methodology to analyze and evaluate the spillover effects. Special attention is paid to selecting an appropriate econometric volatility model. Our results show that the spillover effects often are of a significant magnitude and display considerable variation over time and across commodities. Coal and gas generate non-negligible spillovers during almost the entire sample period. Carbon has very little impact during the early and late parts of the sample, but generates significant, and highly variable, spillovers during the period from 2011 to the end of 2014.

Keywords:
energy markets, skew-Student asymmetric BEKK, time-varying volatility spillovers, volatility impulse response function
JEL: C32, C58, G1, Q41

*Corresponding author. Tel.:+46 70 4500740
Email addresses: rikard.green@eon.se (Rikard Green), karl.magnus.larsson10@gmail.com (Karl Larsson), veronika.lunina@nek.lu.se (Veronika Lunina), birger.nilsson@nek.lu.se (Birger Nilsson)

1. Introduction

In this study, we examine the multivariate modelling of the return series of electrical power, natural gas, coal, and carbon (CO_2) emission allowances in the German market. These commodities are connected through the process of power generation. The prices of the input fuels, namely gas and coal, constitute the main portion of the variable costs of producing electricity. Because the use of gas or coal to produce electricity is associated with carbon emissions, the price of these emissions also enters the cost side of electricity generation. The spread between the power price and the generation cost defines the gross margin of the energy producer. Energy spreads drive the profitability of power plants, and further serve as indicators that provide incentives for agents in the energy sector to invest in future production capacity. For these reasons, it is of fundamental importance that energy companies and policymakers understand how the cost side of the price spreads impacts the electricity price, both in mean and in volatility.

There is a growing body of literature on interrelations between different energy commodities. A common approach in previous research has been to employ methods of co-integration in order to investigate first-order interrelations between different prices. For example, Gjolberg and Johnsen (1999) study crude oil prices. Casassus, Liu, and Tang (2013) provide empirical evidence of co-integration between several petroleum-related markets. A comparable study available for electricity markets is that of De Vany and Walls (1999), who test for co-integration in 11 regional power spot prices in the U.S. market.

All studies mentioned so far are concerned with first-moment interrelations. While second-order interrelations have been extensively studied in the context of equity markets, there are only a few studies related to energy markets. The studies by Lin

and Tamvakis (2001), Efimova and Serletis (2014), and Karali and Ramirez (2014) all examine second-order interrelations in different segments of the U.S. oil and gas markets. Interrelations between crude oil and various other commodities in the European markets are studied in Reboredo (2014) and Liu and Chen (2013). Koenig (2011) studies the time variation in the correlations among power, fuels, and carbon in the U.K. market. Similar to our study, Le Pen and Sevi (2010) use a VAR-BEKK model and employ volatility impulse response functions in their analysis. However, they investigate spillover effects between different regional electricity markets in Europe, and are not concerned with cross-commodity effects.

To the best of our knowledge, this is the first comprehensive study of volatility spillover effects from fuel and carbon prices to power prices in the German market. We focus on the German market for two reasons. Firstly, it represents the largest European power market, which exhibits a growing degree of transparency and openness towards the surrounding markets, with relevant price data being reliable and publicly available from the European Energy Exchange (EEX). The German power market should not necessarily be regarded as a market bounded by national borders since it is a part of the German-Austrian market area, which also includes the suppliers on the Austrian side. Germany further has significant cross-border electricity import-export with many of its neighboring countries, which adds to the degree of competition and openness in the market. The second reason to why we choose to focus on the German market is that it is currently undergoing a structural transition of its energy portfolio in order to reduce its dependence on fossil fuels, moving towards a larger proportion of renewable energy sources. In this study, we thoroughly analyze the volatility spillover effects from fossil fuels and carbon prices to power prices in the light of the ongoing structural changes in the market.

In order to perform the analysis in a reliable and statistically robust way, we

employ a vector autoregressive (VAR) system coupled with time-varying volatilities and correlations, as captured by a relatively general BEKK specification. The VAR part of the model allows for commodity interrelations in expected returns, while the BEKK part of the model allows for interrelations and spillover effects among volatilities and correlations. We estimate the model with six different covariance specifications, each under seven different distributional assumptions, by making use of the flexible skew-Student distribution proposed in Bauwens and Laurent (2005). The flexible distributional assumption allows each return series to have individual statistical properties. Within this model framework, we perform an extensive analysis of the model specification, with particular focus on the specification of conditional second moments and distributional assumptions. According to likelihood tests, the preferred covariance matrix specification is the most general one, allowing for spillover effects across a number of different channels. The tests reject models that do not allow for spillover effects. The preferred distributional specification is also the most general one, allowing for individual skewness and degrees of freedom parameters.

We continue the paper with an economic analysis of the implications using the best model chosen by our specification tests. Our analysis focuses on spillover effects and, for this purpose, we utilize the volatility impulse response function (VIRF), which is an informative and convenient tool for analyzing shock transmission in non-linear systems. Our implementation is based largely on the methodologies in Koop et al. (1996) and Hafner and Herwartz (2006). Similar to Hafner and Herwartz (2006), we refer to large independent and exogenous shocks as *news*. In our analysis we study the impact of news of a magnitude that the markets experience two or three trading days per year on average. Further, we suggest a novel way of normalizing the variance responses, which facilitates comparability both over time and across different commodities.

The VIRF analysis is developed along several dimensions. We investigate how news in the gas, coal and carbon markets affect the expected power market volatility on each trading day from the beginning of 2008 until the end of 2015. First of all, we compute the average responses in power variance for each year. Secondly, we examine the responses for different horizons. Lastly, we are able to differentiate between the effects of news leading to price increases (*positive news*) and news leading to price decreases (*negative news*), which we find highly relevant.

The results show that positive news in gas and coal generate economically significant volatility spillovers to power. On the other hand, negative news in gas and coal have only weak effects. Both positive and negative news in carbon generate significant spillovers to power only during 2011–2014, the period of elevated carbon market volatility. Overall, there is considerable variation in the strength of the spillover effects, both over time and across the markets. Spillovers from gas start to decline both in magnitude and variability in 2011, turning negative in 2013. This is consistent with the developments in the underlying market, where we observe that gas plays a less important role in the generation mix and that clean spark spreads turn negative, in addition to gas market volatility being very low. From 2014 positive news in gas again starts to generate significant spillovers to power volatility, which might be related to the drop in global oil prices, and the associated drop in gas prices, leading to an upward trend in spark spreads and increase in competitiveness of gas-fired power plants. Average spillovers from positive news in coal remain above zero in all years, peaking in 2008 and 2015, when coal market volatility is at the highest levels.

The remainder of this paper is organized in five sections. Our data are presented in Section 2. Sections 3 and 4 describe the model framework and the estimation procedures, respectively. The estimation results and analysis are discussed in Section

5, and Section 6 concludes the paper.

2. The data

Our data set comprises the daily closing prices of the following front-year futures contracts:

1. German base load power, traded on the EEX in EUR/MWh. Base load profile refers to the delivery of power as a constant flow during the delivery period.
2. Gas TTF,[1] traded on the APX-ENDEX exchange in EUR/MWh.
3. Coal API2,[2] traded on the EEX in USD/t. We use the spot USD/EUR exchange rate to convert the prices into EUR/t.
4. CO_2 EU Allowances, traded on the EEX in EUR/t. One EUA permits the emission of one ton of carbon dioxide. The futures contract size is 1000 EUAs.

Since we are concerned with analyzing the interaction between power and fuels in the futures market we require market based daily fuel price references being continuously traded and immediately interacting with the power market. The TTF market meets all of these requirements. According to ICIS, being a leading market information provider, TTF is the most liquid gas market in the region, and it is widely used as a reference for German gas prices. This is furthermore confirmed by market information providers Platts and Heren who use the TTF price as a standard price reference in the daily price reports on German spark spreads. Similar to the case of gas, we require a liquidly traded forward looking price reference for coal that

[1] The Title Transfer Facility (TTF) is a virtual market place for natural gas in the Netherlands.

[2] API2 is a price index calculated as the average of the Argus cif (cost, insurance, and freight), ARA (Amsterdam, Rotterdam, and Antwerpen) assessment, and McCloskey's northwest European steam coal marker.

immediately interacts with the German power market. The API2 price is commonly marketed by the leading market information providers (ICIS, Platts, and Heren) as the relevant coal price reference in Germany. It is furthermore used in the German OTC market for pricing of dark spreads and in daily price assessment reports distributed by market information providers. The CO_2 EU allowances traded on the EEX are also used for pricing the so-called clean spreads, and there is no traded alternative.

The futures prices are sampled daily, and are organized in the rolling contract form. The front-year futures contracts are traded until the last trading day of a year for the delivery of the underlying over the next calendar year. Our sample starts on January 3, 2008, and ends on March 31, 2016. The choice of the starting point is related to the specifics of the carbon EUA market. The European Emissions Trading Scheme (EU ETS) was introduced in 2005 and had to be implemented in three phases, or three trading periods. The first phase (2005–2007) was highly volatile and, during this period, prices could triple or collapse by a half over a one-week period. In 2007, carbon prices fell to almost zero, compared to a peak level of around 30 EUR/t, when it became known that the aggregate emissions were in fact lower than the number of allowances issued. The carbon derivatives market was highly illiquid until the beginning of the second phase in 2008. The daily futures settlement prices for the first phase are available, but there were no actual trades on most of these days. Therefore, we choose to start our sample in 2008. The carbon market is still extremely volatile, and has exhibited a number of sharp rises and falls, not only in the early stages. For example, on April 16, 2013, the price of a yearly carbon futures contract dropped by 42%, from 4.97 EUR/t to 3.25 EUR/t. This happened after the European Parliament rejected a proposal to delay the sales of 900 million EUAs as a supply restriction measure, which was supposed to artificially raise the price during

the period of economic slowdown and the drop in power production. Extreme price movements and high volatility have been characteristic features of the carbon market, and will likely remain so unless there are significant regulatory changes, such as, for example, price caps and floors. Therefore, we keep the extreme observations in our sample, and take their presence into account in the estimations.

Table 1 presents the descriptive statistics for the daily log-returns on our futures contracts. The returns resulting from rolling to a new contract are deleted from the sample.

INSERT TABLE 1 HERE - descriptive statistics

Table 1 shows that all the series are leptokurtic, with the carbon returns being the most extreme case. It is worth noting that we have both positively and negatively skewed series in our sample; the gas and power returns are positively skewed, while coal and carbon returns feature a negative skew. These observations motivate us not only to introduce asymmetry, but also to employ flexible distributional assumptions that allow for different properties of the individual series.

Figure 1 indicates that all return series exhibit time-varying volatility and volatility clustering. The energy markets were not unaffected by the financial crisis and, as can be seen in Figure 1, the gas, power, and coal markets experienced a period of particularly high volatility from the middle of 2008 to the middle of 2009. We can see a slump in gas volatility during 2011–2013, when European hub prices were loosely tracking oil-indexed contract prices in a benign market environment. In 2014, however, the gas market broke out of the relatively stable state, as the sharp fall in the hub prices, as well as uncertainty about future price levels, caused volatility to rise. The coal market experienced an increase in volatility in 2015, as coal demand in Europe declined under pressure of the excess supply of ecologically cleaner cheap

gas. The carbon market features several periods of pronounced volatility. Perhaps the most striking price changes occurred during the first half of 2013, which includes the turmoil caused by the aforementioned decision by the European Parliament not to delay EUA sales.

INSERT FIGURE 1 HERE - log-returns

3. Model framework

This section describes the econometric specification that we use to analyze the volatility dynamics of the energy futures markets. It consists of three building blocks: the model for conditional mean equations, the conditional covariance model, and the choice of the distribution of innovations.

A general model within our multivariate framework can be formulated as follows:

$$r_t = \mu_t + \varepsilon_t, \tag{1}$$

where r_t is a $k \times 1$ vector of log-returns for k different assets, μ_t is a $k \times 1$ conditional mean vector, and ε_t is a $k \times 1$ vector of zero-mean error terms with conditional covariance matrix H_t. Below we discuss each component of the model in more detail.

3.1. Conditional mean

The conditional mean vector is modelled within the vector autoregression (VAR) framework. That is, each return series is assumed to be a linear function of its own past lags and the past lags of the other return series. An unrestricted VAR(p) model (lag order p) can be written as follows:

$$\mu_t = \eta + \Phi_1 r_{t-1} + \ldots + \Phi_p r_{t-p}, \tag{2}$$

where Φ_j, for $j = 1, \ldots, p$, are $k \times k$ matrices and η is a $k \times 1$ vector of constants.

3.2. Conditional covariance

We assume that the conditional covariance matrix H_t follows a multivariate GARCH process of the BEKK type developed by Engle and Kroner (1995) and Kroner and Ng (1998):

$$H_t = C'C + A'\varepsilon_{t-1}\varepsilon'_{t-1}A + B'H_{t-1}B + D'\zeta_{t-1}\zeta'_{t-1}D, \tag{3}$$

where A, B, C, and D are $k \times k$ matrices, ε_{t-1} is the $k \times 1$ vector of error terms in Eq. (1), and ζ_{t-1} is a $k \times 1$ vector of asymmetric error terms. Each element in $\zeta_{t-1} = (\zeta_{1,t-1}, \ldots, \zeta_{k,t-1})$ is defined either as:

$$\zeta^{+}_{i,t-1} \equiv \max(\varepsilon_{i,t-1}, 0) \quad \text{or} \quad \zeta^{-}_{i,t-1} \equiv \min(\varepsilon_{i,t-1}, 0), \tag{4}$$

depending on whether the conditional variance is higher following a positive or a negative shock. We determine the specification of ζ by estimating univariate GARCH models with asymmetric residuals on each individual time series. This approach enforces consistency between the individual series in both the multivariate and univariate models.

The specification of the $k \times k$ parameter matrix C is such that $C'C$ is guaranteed to be positive semi-definite, while A, B, and D are, apart from identifiability conditions, unrestricted $k \times k$ parameter matrices.[3]

We estimate six different versions, M1–M6, of the BEKK model, which are summarized in Table 2. The models differ in terms of the specification of the parameter matrices A, B, and D, and whether or not the asymmetric term (D) is included. The least complex parameterization is M1, in which the parameter matrices A and B

[3] A sufficient condition to eliminate observationally equivalent structures is to fix the sign of one of the diagonal parameters in A, B, and D (see Engle and Kroner, 1995; Kroner and Ng, 1998).

are diagonal matrices, and the asymmetric term is not included. The most complex specification is M6, in which the parameter matrices A, B, and D are non-diagonal, non-symmetric matrices (i.e., with no restrictions on the elements), and where the asymmetric term is included. By definition, diagonal specifications allow for own-market influences on conditional volatility only, while non-diagonal specifications also allow for cross-market influences. If the parameter matrices are symmetric, spillovers between two markets are automatically the same in both directions, while non-symmetric parameter matrices remove this restriction.

INSERT TABLE 2 HERE - covariance specifications

An important feature of the BEKK parameterization is that variances and covariances are modelled directly. Consequently, off-diagonal elements in the parameter matrices A, B, and D have immediate interpretations in terms of cross-market volatility spillover effects. The *signs* of the off-diagonal parameters do not have a straightforward interpretation, because these parameters appear in several non-linear terms determining each element of the H-matrix at each time point. As a result, the total effect of a shock in one market on the volatility in another market is a non-linear function of the shocks to all variables in the system.

3.3. Distributional assumptions

The model framework is completed with a specification of the joint distribution for the vector of error terms ε in Eq. (1). A common practice is to use the multivariate normal distribution and argue that, even if the true conditional distribution of the innovations is not normal, the quasi-maximum likelihood (QML) estimator is consistent and asymptotically normal, provided that the conditional mean and conditional variance equations are correctly specified (see Bollerslev and Wooldridge,

1992). However, Engle and Gonzales-Rivera (1991) show that the QML estimator is inefficient and, furthermore, that its inefficiency increases with the degree of departure from normality. This point is particularly important for financial assets, the returns of which are generally skewed and leptokurtic. Furthermore, in many practical applications that involve estimating tail quantiles, distributions that incorporate non-zero skewness and excess kurtosis are highly relevant, for example, in parametric value-at-risk estimations (see Giot and Laurent, 2003; Hung, Lee, and Liu, 2008; Cheng and Hung, 2011). Therefore, while the normal distribution may serve as a benchmark case, we believe that more flexible distributions are an important building block when modelling energy-related asset returns. In this study, we choose to deviate from the normality assumption. In particular, we implement the VAR-BEKK process in conjunction with the multivariate skew-Student density of Bauwens and Laurent (2002, 2005).

The most general version of the multivariate skew-Student distribution is constructed such that the univariate marginal distributions are allowed to have individual skewness coefficients and different tail properties. Given the nature of our data, summarized in Table 1, with the carbon return series being considerably more leptokurtic, we want to relax the restriction of equal degrees of freedom implied by the standard multivariate Student distribution. We also want to allow for different skewness coefficients of the individual series, especially since we have both positively and negatively skewed variables in our sample. The multivariate skew-Student density with independent components of Bauwens and Laurent (2002, 2005) introduces the above-mentioned flexibilities at a reasonable computational cost. In addition, this skew-Student distribution is relatively straightforward to augment with GARCH-type second-moment dynamics. Naturally, the skewness coefficients, as well as the degrees of freedom, can be restricted to a single value, creating different types

of nested distributions, the relevance of which can be statistically contrasted using standard likelihood ratio tests.

Following Bauwens and Laurent (2002), a $k \times 1$ random vector z_t is said to be standard multivariate skew-Student distributed with independent components if its probability density function is given by:

$$f(z_t) = \left(\frac{2}{\sqrt{\pi}}\right)^k \left[\prod_{i=1}^{k} \frac{\xi_i s_i}{1+\xi_i^2} \frac{\Gamma\left(\frac{\upsilon_i+1}{2}\right)}{\Gamma\left(\frac{\upsilon_i}{2}\right)\sqrt{\upsilon_i-2}} \left(1+\frac{\kappa_{i,t}^2}{\upsilon_i-2}\right)^{-\frac{1+\upsilon_i}{2}}\right], \tag{5}$$

where

$$\kappa_{i,t} = (s_i z_{i,t} + m_i)\, \xi_i^{-I_{i,t}}, \tag{6}$$

and

$$I_{i,t} = \begin{cases} 1 \text{ if } z_{i,t} \geq -\frac{m_i}{s_i} \\ -1 \text{ if } z_{i,t} < -\frac{m_i}{s_i} \end{cases}, \tag{7}$$

with skewness parameters $\xi = (\xi_1, ..., \xi_k)$ and degrees of freedom parameters $\upsilon = (\upsilon_1, ..., \upsilon_k)$, for $\upsilon_i > 2$. We let $\Gamma(x)$ denote the Gamma function evaluated at $x > 0$. The density function $f(z_t)$ is obtained by taking the product of k independent skew-Student components, thereby allowing each marginal distribution to have a different tail behavior. In the present setting, we define the multivariate skew-Student distribution for the vector of standardized residuals z_t as follows:

$$z_t = H_t^{-1/2} \varepsilon_t, \tag{8}$$

where ε_t is the vector of error terms from the model in Eq. (1) and H_t is the BEKK covariance matrix in Eq. (3). The constants $m_i = m_i(\xi_i, \upsilon_i)$ and $s_i = s_i(\xi_i, \upsilon_i)$ are the means and standard deviations of the non-standardized univariate skew-Student density of Fernandez and Steel (1998), respectively, defined by:

$$m_i(\xi_i, \upsilon_i) = \frac{\Gamma\left(\frac{\upsilon_i-1}{2}\right)\sqrt{\upsilon_i-2}}{\sqrt{\pi}\Gamma\left(\frac{\upsilon_i}{2}\right)} \left(\xi_i - \frac{1}{\xi_i}\right), \tag{9}$$

$$s_i^2\left(\xi_i, \upsilon_i\right) = \left(\xi_i^2 + \frac{1}{\xi_i^2} - 1\right) - m_i^2. \tag{10}$$

The parameter ξ_i^2 is the ratio of probability masses above and below the mode, and can be interpreted directly as a measure of skewness. In the case where $\xi_i < 1$, the data are negatively skewed, and $\xi_i > 1$ indicates positive skewness. The symmetric case corresponds to $\xi_i = 1$, which implies that $m_i = 0$ and $s_i = 1$. If we restrict all ξ_i to be equal to 1, and all υ_i to be the same, Eq. (5) reduces to a distribution similar to the textbook multivariate Student density.

4. Estimation

In our final four-asset model framework, we organize the vector of futures log-returns as $r_t = (r_{1,t}, r_{2,t}, r_{3,t}, r_{4,t})'$, where $r_{1,t}$ denotes the return on power, $r_{2,t}$ denotes the return on natural gas, $r_{3,t}$ denotes the return on coal, and $r_{4,t}$ denotes the return on carbon.

We start by determining the appropriate lag-order p for the VAR part governing the conditional mean equation. To do so, we employ a number of different criteria. Individual correlograms of the return series indicate that autocorrelation is present at the first lag, and in some cases, at the second lag as well. We do not observe any weekly seasonal patterns, which in the case of futures contracts traded five days per week would correspond to a correlogram spike at the fifth lag. Next, we compare the VAR models of up to the fifth order based on the information criteria (AIC, SIC and HQ), the sequential likelihood ratio (LR) test statistics, and the final prediction error.[4] Two lags are selected by three out of these five criteria, and none are in favor of more than two lags. The final check is a test for any remaining serial correlation in the

[4]These VAR models are estimated under the assumption of normally distributed innovations.

residuals. According to the multivariate LM test, we can reject the null hypothesis of no autocorrelation up to the second order in residuals of VAR(1), at any conventional significance level. In contrast, for the VAR(2) model, we cannot reject the hypothesis of no autocorrelation up to the second order at the 5% significance level. Therefore, we choose a VAR(2) specification for the conditional mean process.

To determine an appropriate definition for the asymmetric error term of each asset, ζ_i, we estimate univariate GARCH models of the type proposed in Glosten, Jagganathan, and Runkle (1993) for each of the series. Then, we pick the best specification based on the likelihood value. This analysis leads us to specify the vector ζ as:

$$\zeta_t = \left(\zeta_{1,t}^-, \zeta_{2,t}^+, \zeta_{3,t}^+, \zeta_{4,t}^-\right)',$$

where $\zeta_{i,t}^+$ and $\zeta_{i,t}^-$ are defined in Eq. (4). This specification is consistent with the conditional variance being higher after a negative shock for power and carbon, but higher after a positive shock for gas and coal.

4.1. Methodology

We estimate all parameters in our models simultaneously using a full-information maximum likelihood (ML). Our estimation methodology proceeds in three steps. First, we use the OLS method to estimate the parameters in the mean equations, ignoring the GARCH error structure. Then, we estimate the GARCH parameters by QML, assuming normality and conditioning on the given VAR parameters. These two steps yield consistent estimates of all mean and covariance parameters (Bollerslev and Wooldridge, 1992). However, to obtain efficient estimates, a joint estimation of all parameters is required. This motivates our final step, in which all parameters are re-estimated using the parameter estimates from the two initial steps as starting

values only.[5] This procedure is implemented for all six covariance specifications in Table 2.

Let θ denote the parameter vector for the full model. Then, the log-likelihood function is given by:

$$\ln L(\theta) = \sum_{t=3}^{T} \left\{ \ln f(z_t) - \frac{1}{2} \ln |H_t| \right\}, \tag{11}$$

where $f(z_t)$ is the probability density function in Eq. (5), T is the number of time-series observations, and $|H_t|$ denotes the determinant of H_t. Note that the summation starts from $t = 3$ because the estimation is conditional on the first two time series observations owing to the VAR(2) specification of the conditional mean equation. The second term in the sum in Eq. (11) is the Jacobian correction term arising in the transformation from z to ε. To evaluate the likelihood function, we calculate the inverse of the square root matrix $H_t^{-1/2}$ in Eq. (8) at each time point using a standard spectral decomposition. We set the initial H_t equal to the sample covariance matrix and the initial values of the residuals ε_0 are set equal to zero.

We estimate the six different BEKK specifications described in Table 2 by maximizing the log-likelihood function in Eq. (11). In addition, each model is estimated under the assumption of the six types of multivariate Student distributions summarized in Table 3. We also estimate all BEKK specifications for the benchmark case of the normal distribution. In the case of normally distributed residuals, the density function in Eq. (11) is replaced by the standardized normal density, obtained as the limiting distribution of $f(z_t)$ when $\xi_i = 1$, as $\upsilon_i \to \infty$.

[5] As starting values for the distributional parameters in the skew-Student distributions, we use $\xi_i = 1$ for all skewness parameters. For the degrees of freedom υ_i , we use either the value corresponding to the average kurtosis of the data series, or the values corresponding to the individual kurtosis of the data series, depending on the specification (see Table 3).

INSERT TABLE 3 HERE - distributions

In total, we estimate 42 different model specifications. The number of conditional mean parameters is always 36. The total number of conditional covariance parameters together with the skewness and shape parameters ranges from 18 in the simplest specification (M1/Normal) to 66 in the most complex specification (M6/Type6). The log-likelihood function is maximized by simulated annealing, which is a derivative-free stochastic search algorithm. The fundamental property of simulated annealing is that it is allowed to accept worse intermediate solutions (downhill moves) while searching for the optimum, which leads to a more extensive exploration of the parameter space and prevents the algorithm from becoming stuck in local optima. In theory, this property also makes the algorithm insensitive to starting values. However, to further increase the chance of identifying the global optimum, we implement a sequential strategy, described above, which involves using consistent QML estimates as starting values. Our particular implementation of the algorithm follows closely the approach in Goffe, Ferrier, and Rogers (1994). The advantages of simulated annealing come at the cost of a higher execution time when compared to conventional algorithms. Thus, we execute all optimizations on a high-performance computer cluster. We calculate the standard errors for individual parameters by estimating the outer product of the gradients matrix using numerical first derivatives.[6]

[6] An alternative is to calculate the standard errors based on the inverse of the Hessian. However, implementing stable and reliable numerical second derivatives is a challenge, even in less complex settings than ours. Thus, we leave this topic for future research.

5. Results

We first describe our preferred model specification. Then, we discuss the estimated parameters from this model, with a particular focus on volatility spillovers. Finally, we conduct an elaborate variance impulse-response (VIRF) analysis to gain further insight into how news of one market (gas, coal, or carbon) propagates through the system to affect the volatility in the power market. In particular, we examine the differences between commodities and changes over time.

5.1. Model specification

The conditional mean equation in our model is a preselected VAR(2) specification. Therefore, the choice of the preferred model involves two parts: the covariance specification and the distributional assumption.

Table 4 reports the results of the LR tests of the six BEKK specifications. We find that, regardless of the additional assumptions, the models with an asymmetric term and with non-diagonal parameter matrices are superior. The results for non-symmetric versus symmetric parameter matrices are more involved. Without the asymmetric term, the spillover effects are the same in both directions (M3 is not rejected against M5). However, when the asymmetric term is included, the spillover effects are not the same in both directions (M4 is rejected against M6).

INSERT TABLE 4 HERE - LR tests covariance

Because specifications with diagonal parameter matrices are rejected against their non-diagonal counterparts, we conclude that there exist volatility spillovers in the energy futures markets. Also, because all models without the asymmetric term are rejected, asymmetric effects in volatility are clearly prevalent in these markets. From the second result above, we infer that these spillovers are the same in both directions

for the symmetric terms (matrices A and B), but that they are different for the asymmetric term (matrix D). In addition, both M1 and M3 are rejected against M6.[7] In summary, based on the LR tests, we prefer the most general covariance model (M6), with non-diagonal, non-symmetric parameter matrices and an asymmetric term.

Next, we compare the distributional specifications using LR tests. The distributional test results for the M6 covariance model are summarized in Table 5.[8] As the first observation (not reported), we note that the log-likelihood value increases significantly when switching from the benchmark normal distribution to the simplest Student distribution (Type1). This indicates that allowing for excess kurtosis is highly important also in a conditional setting, which is not surprising given the descriptive statistics in Table 1 that clearly indicate that energy futures returns exhibit excess sample kurtosis. Furthermore, because the models with equal degrees of freedom are rejected against models that allow for different degrees of freedom (Type1 against Type2, Type3 against Type4, and Type5 against Type6), our results also suggest that the excess kurtosis is statistically different between the four commodities. From Table 1, it is clear that kurtosis of carbon returns is most likely to be the main cause of this result.

INSERT TABLE 5 HERE - LR tests distribution

We reject Type1 against Type3, and Type2 against Type4 (however marginally),

[7] Our focus in the sequel is on M6, which can be tested against all other covariance models and based on these tests is our preferred covariance specification. For this reason we do not investigate the non-nested covariance models further.

[8] The conclusions are the same regardless of the covariance model specification, although we only report the distributional test results for the preferred model M6.

which means that non-zero skewness is statistically important. Allowing for different individual skewness is statistically even more important, because we strongly reject Type3 against Type5, and Type4 against Type6. These results are also not unexpected because from Table 1, two of the commodities have negative sample skewness, and the other two have positive sample skewness, which logically should make it worthwhile to allow for individual skewness. Based on these tests, our preferred distribution is Type6, which is the multivariate skew-Student distribution with both individual skewness and kurtosis (degrees of freedom) for the different energy futures.[9]

All further analysis is based on the estimation results of the preferred model: M6/Type6. In the next section, we examine the significance of the individual parameters, focusing mainly on the parameters directly related to volatility spillovers.

5.2. Parameter estimates

Tables 6 and 7 present the estimation results for the model M6/Type6. We are particularly interested in the off-diagonal elements of the A, B, and D parameter matrices, because they control the cross-market effects in the second-moment dynamics. However, we start with a general overview of the estimation results.

INSERT TABLE 6 HERE - mean parameters

INSERT TABLE 7 HERE - covariance parameters

We find a number of cross-commodity effects in the mean equations. There are particularly many significant parameters in the power mean equation (parameters

[9]Our focus in the sequel is on Type6, which can be tested against all other distribution types and based on these tests is our preferred distribution. For this reason we do not investigate the non-nested distributions further.

$\phi_{12}^{(1)}$, $\phi_{13}^{(1)}$, $\phi_{14}^{(1)}$, and $\phi_{14}^{(2)}$). All diagonal elements of the A- and B-matrices are significant, which confirms the existence of own-market GARCH effects in the volatility dynamics of energy futures log-returns. The diagonal elements of the B-matrix indicate high levels of persistence in volatilities. Among the diagonal elements of the D-matrix, we find d_{11} of power, d_{33} of coal and d_{44} of carbon to be significant. This confirms the presence of asymmetric effects in the conditional volatility of these assets. We find no evidence of any asymmetric effects in the gas volatility for which asymmetric residuals were defined to be positive.

The skewness parameters ξ_1 of power and ξ_2 of gas are statistically significantly larger than 1 at the 5% and 1% levels, respectively. This is consistent with the positive sign of the unconditional skewness in the data.

Of the nine parameters that control volatility spillovers to the power market (a_{21}, a_{31}, a_{41}, b_{21}, b_{31}, b_{41}, d_{21}, d_{31}, d_{41}), we find that a_{21}, a_{41}, d_{21}, and d_{31} are statistically significant. The spillovers associated with these parameters are coming from all the other markets, and are channeled through both regular and asymmetric BEKK terms. Volatility spillovers are determined by combinations of parameters and in Section 5.4 we will investigate these effects with the use of the VIRF methodology.

The interrelation in volatility between electrical power and a specific fuel should in part be related to the profitability of power generation from that fuel type. Based on the comparison of clean dark spreads versus clean spark spreads we find that power generation from coal was more profitable than that from gas during almost the entire sample period.[10] Moreover, coal never fell out-of-the-money, unlike gas, for

[10] We use the following typical definitions of the clean spark spreads (CSS) and clean dark spreads (CDS):

$$\text{CSS} = \text{Power} - 2 \times \text{Gas} - 0.4 \times \text{Carbon},$$

which the clean spark spread became negative from the beginning of 2013 onwards. This competitive advantage of coal versus gas was driven by a relative weakness in coal and carbon prices, while the price level in gas was reinforced by oil linkage. However, the trend reversed in late 2014, after the severe drop in global oil prices, and the associated drop in gas prices.

To gain additional insights, we examine the data on actual daily electricity production in Germany from different technologies, available at the EEX Transparency platform. Much more electricity was generated from coal almost every day during our sample period. Generation levels from gas were steadily falling until the beginning of 2014, owing to decreasing spark spreads. However, during 2014–2016 we observe a reversal of this trend, with gas power plants slowly building up competitiveness in light of the low oil price environment, as well as the recent surplus in the global supply of Liquefied Natural Gas (LNG). We believe that these fundamental relationships in the supply stack must also affect the relative strength of volatility spillover effects in the energy markets.

Finally, we also report statistically significant parameters involved in spillovers between the different fuel components. For instance, we observe a bidirectional statistically significant spillover between the coal market and the gas market (parameters a_{23}, b_{23}, and b_{32}). We believe that an increase in coal volatility impacts the uncertainty of the future production mix (coal/gas) for power production, which manifests as gas volatility, and vice versa. Moreover, we also report statistically significant parameters involved in spillover effects from the coal market to the carbon market

---

and

$$\text{CDS} = \text{Power} - 0.4 \times \text{Coal} - 0.9 \times \text{Carbon}.$$

.

(parameters b_{34} and d_{34}). We note that the coal and carbon markets are clearly linked via the power market, because coal power plants are major CO_2 emitters. In terms of electrical energy, coal emits more than twice as much CO_2 as gas. This is verified by the carbon coefficients in the spark and dark spread definitions (see footnote 10), which represents the number of carbon credits necessary to cover the respective power production. We believe that the connection between the coal and carbon markets, along with coal having been a profitable technology (in-the-money) for power production during the full sample period are why we find significant parameters related to volatility spillover effects from coal to power. An increase in coal volatility likely creates uncertainty about the future production mix (coal/gas) and, hence, uncertainty about future CO_2 volumes, which finally transmits to the carbon prices.

5.3. Conditional correlations

Next, we use the estimated parameters to calculate conditional correlations. This topic is of economic relevance, because correlations reflect the extent to which power and fuel prices move together. This, in turn, determines the hedging strategies of power producers.

Figure 2 presents the power/gas and power/coal correlations obtained from the preferred model (M6/Type6). Being model generated, the estimated day-by-day correlations should be interpreted with care. However, we are only interested in the overall development of the correlations over time as conveyed in Figure 2.

INSERT FIGURE 2 HERE - correlations

The correlations between power and gas display a steady decrease from 2008 until 2013. During this period the clean spark spread has decreased successively and

gas volumes have gradually been reduced from the generation mix. This structural change is related to the increasing share of renewables within the same time horizon, pushing gas out of the merit order as the most expensive fuel. The reduction in gas volumes has likely also contributed to the general trend of decreasing correlations between power and carbon over the same period. The power/gas correlations exhibit a particularly sharp decline from the beginning of 2013, which coincides with the spark spreads turning negative. The negative spark spreads have a direct impact in the gas market where the volumes used for power production are rapidly reduced, which clearly weakens the fundamental connection between power and gas. In the last years of the sample period (2014–2016) the clean spark spread partially returns into the money, and the power/gas correlation increases. Such temporary periods of moneyness most commonly take place during cold winter months, where they are captured by efficient CCGT (combined cycle gas turbine) plants.

To fully understand the evolution of the power/gas correlations we also need to recognize the changes in volatility during the sample period. Between 2008–2013 we observe a decreasing trend in the volatility of gas prices. In periods of low volatility the power plant owners are not required to update their economic generation calculation as often, which means that the hedge positions for plants can be left unchanged for longer periods. This loosens the connection between the power and gas markets. In 2014 we observe a rapid increase in the gas volatility, which lasts for the remainder of the sample period. In connection with this change, the plant owners are likely to adopt a more frequent hedging strategy, which again strengthens the linkage between gas and power and increases the correlation.

Similar to power/gas correlations, power/coal correlations exhibit an overall downward trend until 2014, followed by an upward trend lasting until the end of our sample period. Contrary to the case of gas, the clean dark spread has clearly remained posi-

tive during the whole sample period. The coal price volatility, however, is decreasing from 2011 up until the beginning of 2015, and we therefore argue that the changed hedging behavior of plant owners might have contributed to the observed decrease in correlations. In 2015 the coal volatility increases and plant owners are likely to adopt a more frequent hedging strategy that tightens the connection between power and coal and increases the correlation.

5.4. Variance impulse response analysis

5.4.1. Definition and computation of the VIRF

The volatility impulse response function (VIRF) is a recently developed econometric tool used to understand the dynamics of shock transmission in a non-linear system, which is arguably more informative than considering individual estimated parameters alone. The VIRF concept was introduced by Hafner and Herwartz (2006), who extended the generalized impulse response function of Koop et al. (1996) to a general symmetric multivariate GARCH setting. The VIRF measures the response in the variances and covariances in future periods to *news* in the underlying variables today, for example commodity returns. We consider news in the return of *one* of the commodities, and the corresponding VIRFs describe the transmission or propagation of this news to the variances and covariances of all other commodities over time, through the non-linear BEKK system. Accordingly, the news vector z is a vector with a non-zero element in one position and zero elements elsewhere:

$$
\begin{aligned}
z &= (z_1, 0, 0, 0)' \\
z &= (0, z_2, 0, 0)' \\
z &= (0, 0, z_3, 0)' \\
z &= (0, 0, 0, z_4)' ,
\end{aligned}
$$

where z_i denotes news in the return of commodity $i = 1, ..., 4$; power, gas, coal, and carbon. Note that the news vectors are time invariant, because the individual news processes (i.e., the univariate marginal densities in Eq. (5)) are standardized w.r.t. the mean and the variance, and have constant higher moments. We consider the 99% and the 1% quantiles in the news distributions, which we refer to as positive news and negative news, respectively.[11] Therefore, the markets, on average, experience news of this magnitude two or three trading days per year, both for positive and negative news. Positive news corresponds to an increase in a commodity price, while negative news represents a price decrease. We separate news and shocks conceptually, and the shock ε_t corresponding to news z is given by:

$$\varepsilon_t = H_t^{1/2} z = (\varepsilon_{1t}, \varepsilon_{2t}, \varepsilon_{3t}, \varepsilon_{4t})', \tag{12}$$

where $H_t^{1/2}$ is the "square root" of the covariance matrix, calculated using the spectral decomposition. In general, all elements in ε_t are time-varying and non-zero because of the dependence structure imposed by the time-varying and non-diagonal covariance matrix H_t.

The VIRF defined in terms of the shock ε_t is given by:

$$VIRF\left(t, n, \omega_{t-1}, \varepsilon_t\right) = E\left[vech(H_{t+n})|\omega_{t-1}, \varepsilon_t\right] - E\left[vech(H_{t+n})|\omega_{t-1}\right], \tag{13}$$

where $vech()$ is the operator that stacks the lower triangular fraction of a $k \times k$ matrix into a $k^* = k(k+1)/2$ dimensional vector. The first expectation in Eq. (13)

[11] The model-implied 99% quantiles (positive news) are $z_1 = 3.206$, $z_2 = 3.180$, $z_3 = 2.841$ and $z_4 = 3.357$. The 1% quantiles (negative news) are $z_1 = -2.905$, $z_2 = -2.671$, $z_3 = -2.887$ and $z_4 = -3.596$. The 99% quantile for a given commodity is numerically different from the 1% quantile because of the estimated non-zero skewness. Power and gas are right-skewed and, therefore, the 99% quantile is larger in absolute terms than the 1% quantile. For coal and carbon the opposite is true.

is the expected covariance matrix n periods ahead, given the history ω_{t-1} (i.e., all previous shocks) and the time t shock ε_t. The second expectation is the expected covariance matrix n periods ahead, given only the history (the baseline expectation). In our case of four commodities, the VIRF as given by Eq. (13) is a 10×1 vector, with four entries representing the responses in variances and six entries representing the responses in covariances. Note that the shock enters the covariance process non-linearly. Therefore, the baseline expectation does not correspond to a zero shock (i.e., ε_t equal to the zero vector). In the definition of the VIRF, future shocks are not zero and, therefore, the effect of future shocks is averaged out in the calculation of the VIRF.

To evaluate the expectations, Hafner and Herwartz (2006) derive an analytical expression of the VIRF for symmetric BEKK models. However, our preferred model is an asymmetric BEKK model that lacks analytical expressions for the expectations. Therefore, we perform the integrations numerically using the Monte Carlo method instead, following the procedure outlined in Koop et al. (1996) for computation of the generalized impulse response function. We draw from the underlying univariate skew-Student distributions to generate future scenarios (shocks), using the analytical quantile function.

To calculate the VIRFs, we proceed in two steps:

1. Construct shocks ε_t for each trading day t, corresponding to positive and negative news z_i for each commodity. This gives two time-series of shocks for each commodity (in total, eight time-series of shocks).

2. Calculate a VIRF for each trading day t for each time-series of shocks.

In step two, given the constructed shocks for both positive and negative news, we calculate the VIRFs at each trading day t for all commodities, and for horizons from $n = 1$ to $n = 63$ (i.e., approximately three calendar months ahead). We average

out the future shocks over $20,000$ simulated trajectories.[12] Finally, we normalize the variance responses for all commodities with the initial baseline expected own variance (i.e., the baseline expectation one period ahead). This normalization creates a "percentage" response in the variances that is comparable over time and across commodities.

5.4.2. Results of the VIRF analysis

We focus our empirical analysis on the transmission of news in gas, coal, and carbon to the variance of power. Thus we are primarily interested in a single element of the VIRF vector, which we refer to as the power VIRF, or simply the VIRF, in this subsection.

We present two sets of complementing results, based on the calculations outlined above. First, we show the average variance response in power for each year, 2008 to 2015, for all horizons. The yearly VIRFs are calculated by taking the average of the daily VIRFs over all trading days each year. This yearly analysis gives an overall dynamic picture of the strength of volatility spillovers between the different commodities. It also provides us with insights into the speed of decay of the responses when the horizon increases. Second, we show the initial day-ahead responses in power variance for each trading day in the sample. This daily time series analysis gives a different picture of the time variation in the news transmission, which allows us to trace changes in the volatility spillovers over time in more detail, and to connect these changes to specific market events.

[12] We calculate a VIRF for each trading day from January 7, 2008 to December 29, 2015, when there are 63 trading days remaining in the sample. We cannot iterate the BEKK model outside the sample, because we need the actual covariance matrix to construct the shocks (futures), given the simulated news.

The yearly VIRFs are plotted in Figures 3–5. These plots provide us with insight into the nature of the spillover effects from various perspectives. First, we can track changes over time. Second, since the normalized VIRFs are expressed as percentages, we can compare the strength of the news transmission between different commodities in a more straightforward way than by examining the estimated coefficients. It is also possible to determine the half-life of a shock and assess how fast the system recovers after an abnormal event. Finally, we can differentiate between the impact of positive and negative news.

Econometrically, these varying volatility responses are a consequence of the complex dynamic interrelations between the different commodities in the BEKK system. By construction of the VIRF, the strength of volatility spillovers is directly proportional to the level of volatility and correlations in the underlying markets. This also makes sense intuitively, since we would expect larger spillovers to occur at more turbulent times, as well as between highly correlated markets. Figures 3 and 4 reveal how the impact of news in gas and coal prices on power price variance changes depending on relative volatility levels in these markets, as well as their correlation with the power market. Coal news leads to larger responses in power price variance, compared to gas news, in 2008, 2012, 2013, and 2015. For example, in 2015, positive news in the coal market results in an, on average, 23% larger than otherwise expected day-ahead variance in the power market, compared to the corresponding effect of 14% for positive news in the gas market. Note that in 2013, when the period of the lowest power/gas correlations coincides with subdued gas volatility, we find a negative power VIRF in response to positive gas news. Technically, a negative VIRF means that the expected power variance, given the news in gas, is lower than what we would otherwise expect it to be. Economically, this reveals weakness of the fundamental production link between power and gas markets during that period, which

is in line with clean spark spreads reaching their lowest, and the associated drop in the competitiveness of gas-fired power plants.

INSERT FIGURES 3-5 HERE - yearly VIRFs

Further, we find that the response in power variance is much larger following positive news than following negative news in both gas and coal throughout the sample period. This result makes sense, because increases in the prices of fuels, such as gas or coal, have a negative effect on the profit margins of power producers. For carbon, the story is different. There are no large differences in the responses to positive and negative news. We see no significant difference during 2008–2011, while starting from 2012, negative news has a slight tendency to produce higher VIRFs. However, it is only during 2011–2014 that carbon news leads to economically significant spillovers. This increase in spillovers from carbon may be explained by a significant increase in carbon price volatility during that period. However, the underlying economic reasons for the patterns we see in response to positive and negative carbon news are much harder to identify.

We find news in gas to have a longer-lasting effect, on average, than news in coal. It takes approximately ten trading days for a power VIRF to decrease by half after news in gas, compared to eight trading days after news in coal. News in carbon has the least lasting effect on expected power volatility, with an average half-life of five trading days.

Figure 6 displays the evolution of the day-ahead responses in the power variance over the sample period, providing a detailed dynamics behind the average day-ahead responses corresponding to $n = 1$ points on Figures 3–5. The spillovers to the power variance resulting from news in all other commodities show considerable variation over time. Figure 6 shows that day-ahead increases in the expected power variance

following positive news in coal range between 0% and 20%, in most years, with generally higher levels in 2008 and 2015. The day-ahead responses to positive news in gas are at the highest levels in the second half of 2009, averaging at roughly 35%, followed by a steady decrease during 2011–2013, and a revival in the end of our sample period. The lower, right panel on Figure 6 indicates that positive news in the power market itself leads to, on average, 20% higher than expected power price variance, while the impact of own negative news is slightly lower. In comparison to these levels, the cross-market effects depicted on the rest of the panels are far from trivial.

INSERT FIGURE 6 HERE - daily VIRFs

Another perspective of the strength of the spillover effects is provided by calculating the "critical news" at time t required to generate a VIRF of zero at time $t+1$. How large does news in gas, coal, and carbon have to be to obtain a VIRF of zero? Recall that a VIRF of zero means a variance response in power that is equal to the baseline expected power variance. These critical news levels have to be calculated numerically, and we do so for both positive (right-tail) and negative (left-tail) news. We report the results as critical quantiles rather than actual news values because this gives a more direct sense of the magnitude of news required to generate a VIRF of zero. These quantile values can also be related to the 99% and 1% quantiles we used in our previous VIRF calculations. The results are reported in Table 8, where we list the positive and negative quantiles (as percentages) for all commodities and for each year in our sample. We observe that the news that makes the VIRF at $t+1$ equal to zero varies significantly across commodities and over time. For example, extremely large positive and negative news is required in gas in 2013 (at the 99.58% quantile in the right tail and the 0.01% quantile in the left tail). News at the 99% quantile, used

to calculate the VIRFs presented earlier in this section, are not sufficient to produce a positive power variance response. On the other hand, for carbon in 2013, news at the 96.63% level in the right tail and 4.69% in the left tail are sufficient.

INSERT TABLE 8 HERE - critical quantiles

6. Summary and conclusions

In this study, we investigate the transmission of news and volatility spillovers between electrical power, gas, coal, and carbon in the German market. The price of power is connected to the prices of gas, coal, and carbon through the cost of electricity generation (gas, coal) and emissions (carbon). Our sample data consist of futures prices for power, gas, coal, and carbon emission allowances for the period from January 2008 to March 2016. We study the spillover effects that news originating in the gas, coal, and carbon markets have on the variance of power.

In the analysis, we estimate a four-asset VAR-BEKK model that allows for spillover effects through several different channels. To measure and evaluate the strength of spillovers from different commodities and during different periods, we use the volatility impulse response function (VIRF) as our primary tool. From the estimation and analysis of VIRFs, we conclude that there are significant spillover effects from gas, coal, and carbon affecting the variance of power. The results indicate that spillover effects show large variation across commodities and over time. Spillovers from coal are substantial throughout our sample period, but with significant time variation on a daily basis. Spillovers from gas are also substantial during 2008–2010, after which they start to decrease in magnitude and turn negative for the majority of 2013. This coincides with the period of low gas market volatility, low power/gas correlations, and unprofitability of gas-fired power plants as measured

by spark spreads. However, in 2014 we see a revival of spillover effects from gas to power, as gas prices fall in the low oil price environment, increasing the competitiveness of gas versus coal as a power generation fuel. We find that it takes longer, on average, for the effect of news in gas to die out, compared to the effect of news in coal. Spillovers from carbon exhibit the fastest decay and are economically significant between 2011 and 2014, which is the period of highest volatility in the carbon market. We find that positive news in gas and coal markets leads to a much larger response in the variance of power compared to negative news. Distinguishing between positive and negative news appears to be much less important for the carbon market.

There are a number of interesting applications that could be explored within our multivariate framework in future studies. Risk management applications such as hedging and Value-at-Risk calculations for different portfolios of energy assets appear particularly relevant in this setting. Physical gas- and coal-fired power plants, and financial spark- and dark-spread positions are natural examples of such portfolios.

Acknowledgements

The authors wish to thank two referees, as well as conference discussants and participants at the Energy and Commodity Finance Conference 2016, Commodity Markets Conference 2016 and Stochastics in Financial and Environmental Economics 2014, for their comments and suggestions, which helped to significantly improve this paper. Discussions with the quantitative analysts and traders at E.ON Global Commodities (Düsseldorf) contributed to the development of this study. The computations were performed on resources provided by the Swedish National Infrastructure for Computing at LUNARC, Lund University. Financial support from the Knut Wicksell Centre for Financial Studies at Lund University and the Marianne and Marcus Wallenberg foundation is gratefully acknowledged.

References

[1] Bauwens, L., Laurent, S., 2002. A new class of multivariate skew densities, with applications to GARCH models. CORE Discussion Paper 20.

[2] Bauwens, L., Laurent, S., 2005. A new class of multivariate skew densities, with application to Generalized Autoregressive Conditional Heteroscedasticity models. Journal of Business and Economic Statistics 23, 346–354.

[3] Bollerslev, T., Wooldridge, J. M., 1992. Quasi-maximum likelihood estimation and inference in dynamic models with time-varying covariances. Econometric Reviews 11, 143–172.

[4] Casassus, J., Liu, P., Tang, K., 2013. Economic linkages, relative scarcity, and commodity futures returns. Review of Financial Studies 26, 1324–1362.

[5] Cheng, W.-H., Hung, J.-C., 2011. Skewness and leptokurtosis in GARCH-typed VaR estimation of petroleum and metal asset returns. Journal of Empirical Finance 18, 160–173.

[6] De Vany, A.S., Walls, W.D., 1999. Cointegration analysis of spot electricity prices: insights on transmission efficiency in the western US. Energy Economics 21, 435–448.

[7] Efimova, O., Serletis, A., 2014. Energy markets volatility modelling using GARCH. Energy Economics 43, 264–273.

[8] Engle, R., Gonzalez-Rivera, G., 1991. Semiparametric ARCH Model. Journal of Business and Economic Statistics 9, 345–360.

[9] Engle, R., Kroner, K., 1995. Multivariate simultaneous generalized ARCH. Econometric Theory 11, 122–150.

[10] Fernandez, C., Steel, M.F.J., 1998. On Bayesian modelling of fat tails and skewness. Journal of the American Statistical Association 93, 359–371.

[11] Giot, P., Laurent, S., 2003. Value-at-Risk for long and short positions. Journal of Applied Econometrics 18, 641–664.

[12] Gjolberg, O., Johnsen, T., 1999. Risk management in the oil industry: can information on long-run equilibrium prices be utilized? Energy Economics 21, 517–527.

[13] Glosten, L.R., Jagganathan, R., Runkle, D.E., 1993. On the relation between the expected value and the volatility of the nominal excess return on stocks. Journal of Finance 48, 1779–1801.

[14] Goffe, W., Ferrier, G., Rogers, J., 1994. Global optimization of statistical functions with simulated annealing. Journal of Econometrics 60, 65–99.

[15] Hafner, C.M., Herwartz, H., 2006. Volatility impulse responses for multivariate GARCH models: An exchange rate illustration. Journal of International Money and Finance 25, 719–740.

[16] Hung, J.C., Lee, M.C., Liu, H.C., 2008. Estimation of Value-at-Risk for energy commodities via fat-tailed GARCH models. Energy Economics 30, 1173–1191.

[17] Karali, B., Ramirez, O.A., 2014. Macro determinants of volatility and volatility spillover in energy markets. Energy Economics 46, 413–421.

[18] Koenig, P., 2011. Modelling correlation in carbon and energy markets. Cambridge Working Paper in Economics 1123.

[19] Koop, G.M., Pesaran, H.M., Potter, S.M., 1996. Impulse response analysis in nonlinear multivariate models. Journal of Econometrics 74, 119–147.

[20] Kroner, K., Ng, V., 1998. Modeling asymmetric comovements of asset returns. Review of Financial Studies 11, 817–844.

[21] Le Pen, Y., Sevi, B., 2010. Volatility transmissions and volatility impulse response functions in European energy forward markets. Energy Economics 32, 758–770.

[22] Lin, S.X., Tamvakis, M.V., 2001. Spillover effects in energy futures markets. Energy Economics 23, 43–56.

[23] Liu, H.-H., Chen, Y.-C., 2013. A study on the volatility spillovers, long memory effects and interactions between carbon and energy markets: The impacts of extreme weather. Economic Modelling 35, 840–855.

[24] Reboredo, J.C., 2014. Volatility spillovers between the oil market and the European Union carbon emission market. Economic Modelling 36, 229–234.

Table 1
Summary statistics for log-returns.

	Power	Gas	Coal	Carbon
Mean (%)	-0.057	-0.059	-0.048	-0.068
Median (%)	-0.062	-0.062	-0.040	0.000
Maximum (%)	6.508	9.224	8.622	22.369
Minimum (%)	-5.909	-7.406	-9.821	-42.477
Std. Dev. (%)	1.011	1.316	1.370	3.150
Skewness	0.156	0.460	-0.211	-1.057
Kurtosis	8.213	7.623	9.099	22.867

Table 2
Conditional covariance specifications.

Model	Parameter matrices A, B, and D	Asymmetric BEKK term
M1	diagonal	no
M2	diagonal	yes
M3	non-diagonal symmetric	no
M4	non-diagonal symmetric	yes
M5	non-diagonal non-symmetric	no
M6	non-diagonal non-symmetric	yes

Table 3
Types of Student distributions.

Parameter	Type 1	Type 2	Type 3	Type 4	Type 5	Type 6
υ_1	υ	υ_1	υ	υ_1	υ	υ_1
υ_2	υ	υ_2	υ	υ_2	υ	υ_2
υ_3	υ	υ_3	υ	υ_3	υ	υ_3
υ_4	υ	υ_4	υ	υ_4	υ	υ_4
ξ_1	1	1	ξ	ξ	ξ_1	ξ_1
ξ_2	1	1	ξ	ξ	ξ_2	ξ_2
ξ_3	1	1	ξ	ξ	ξ_3	ξ_3
ξ_4	1	1	ξ	ξ	ξ_4	ξ_4

Note: Types 1 and 2 correspond to symmetric distributions. Types 3 and 4 are asymmetric with a common value of the skewness parameter, while Types 5 and 6 allow the variables to have different skewness properties. With respect to kurtosis, Types 1, 3, and 5 restrict degrees of freedom parameters to a common value, while Types 2, 4, and 6 allow them to vary.

Table 4
Likelihood ratio tests of covariance specifications.

	Test	5% cr.v.	1% cr.v.	Type 1	Type 2	Type 3	Type 4	Type 5	Type 6
1	M1 vs. M2 LR (4)	9.49	13.28	78.68	75.06	78.73	74.82	79.95	76.84
2	M3 vs. M4 LR (10)	18.31	23.21	114.30	114.18	114.37	113.99	112.29	112.61
3	M5 vs. M6 LR (16)	26.30	32.00	139.70	140.12	140.34	140.31	138.69	139.86
4	M1 vs. M3 LR (12)	21.03	26.22	29.61	28.43	28.85	27.68	27.33	26.17
5	M2 vs. M4 LR (18)	28.87	34.81	65.23	67.54	64.49	66.84	59.67	61.94
6	M1 vs. M5 LR (24)	36.42	42.98	42.43	40.67	41.36	39.48	39.08	37.52
7	M2 vs. M6 LR (36)	51.00	58.62	103.45	105.72	102.97	104.97	97.81	100.54
8	M3 vs. M5 LR (12)	21.03	26.22	12.82	12.24	12.51	11.80	11.74	11.35
9	M4 vs. M6 LR (18)	28.87	34.81	38.21	38.18	38.48	38.13	38.14	38.60
10	M1 vs. M4 LR (22)	33.92	40.29	143.92	142.61	143.22	141.67	139.62	138.78
11	M1 vs. M6 LR (40)	55.76	63.69	182.13	180.79	181.70	179.79	177.76	177.38
12	M3 vs. M6 LR (28)	41.34	48.28	152.52	152.36	152.85	152.11	150.43	151.21

Note: Tests 1–3 are for the asymmetric BEKK term (H_0: $D = 0$ versus H_1: $D \neq 0$).
Tests 4–5 are for H_0: diagonal matrices versus H_1: non-diagonal, symmetric matrices.
Tests 6–7 are for H_0: diagonal matrices versus H_1: non-diagonal, non-symmetric matrices.
Tests 8–9 are for H_0: non-diagonal symmetric matrices versus H_1: non-diagonal, non-symmetric matrices.
Tests 10-12 are for the remaining nested covariance specifications.
The left-out combinations of models are not nested. The degrees of freedom are reported in parentheses. Columns 3 and 4 report the upper-tail critical values of χ^2-distribution with the corresponding degrees of freedom, while columns 5–10 report the LR test statistics.

Table 5
Likelihood ratio tests of distributional specifications for model M6.

LR	Type 1	Type 2	Type 3	Type 4	Type 5	Type 6
Type 1		0.017	0.050	0.007	0.000	0.000
		(dgf=3)	(dgf=1)	(dgf=4)	(dgf=4)	(dgf=7)
Type 2			–	0.044	–	0.000
				(dgf=1)		(dgf=4)
Type 3				0.015	0.001	0.000
				(dgf=3)	(dgf=3)	(dgf=6)
Type 4					–	0.001
						(dgf=3)
Type 5						0.016
						(dgf=3)
Type 6						

Note: '–' indicates that the distributional types are not nested. The table reports the χ^2 p-values for upper-tail one-sided tests with the corresponding degrees of freedom reported in parentheses.

Table 6
Conditional mean parameter estimates for the M6/Type6 model.

η_1	-0.032***	η_2	-0.008	η_3	-0.033	η_4	-0.021
	(0.012)		(0.018)		(0.020)		(0.042)
$\phi_{11}^{(1)}$	-0.068***	$\phi_{12}^{(1)}$	0.041***	$\phi_{13}^{(1)}$	0.024*	$\phi_{14}^{(1)}$	0.027***
	(0.021)		(0.014)		(0.014)		(0.004)
$\phi_{21}^{(1)}$	0.001	$\phi_{22}^{(1)}$	0.053**	$\phi_{23}^{(1)}$	0.003	$\phi_{24}^{(1)}$	0.001
	(0.010)		(0.022)		(0.018)		(0.005)
$\phi_{31}^{(1)}$	0.094**	$\phi_{32}^{(1)}$	0.098***	$\phi_{33}^{(1)}$	-0.029	$\phi_{34}^{(1)}$	-0.004
	(0.037)		(0.023)		(0.025)		(0.006)
$\phi_{41}^{(1)}$	-0.008	$\phi_{42}^{(1)}$	-0.056	$\phi_{43}^{(1)}$	-0.127***	$\phi_{44}^{(1)}$	-0.011
	(0.062)		(0.035)		(0.039)		(0.021)
$\phi_{11}^{(2)}$	-0.036*	$\phi_{12}^{(2)}$	0.020	$\phi_{13}^{(2)}$	0.011	$\phi_{14}^{(2)}$	-0.008*
	(0.020)		(0.014)		(0.014)		(0.005)
$\phi_{21}^{(2)}$	0.000	$\phi_{22}^{(2)}$	0.020	$\phi_{23}^{(2)}$	0.004	$\phi_{24}^{(2)}$	-0.004
	(0.001)		(0.022)		(0.019)		(0.005)
$\phi_{31}^{(2)}$	0.016	$\phi_{32}^{(2)}$	-0.002	$\phi_{33}^{(2)}$	-0.035	$\phi_{34}^{(2)}$	-0.007
	(0.034)		(0.021)		(0.024)		(0.007)
$\phi_{41}^{(2)}$	0.028	$\phi_{42}^{(2)}$	0.084**	$\phi_{43}^{(2)}$	-0.056	$\phi_{44}^{(2)}$	-0.074***
	(0.064)		(0.039)		(0.040)		(0.022)

Note: The conditional mean is given by Eq. (2), where η is a 4×1 vector of constants, and Φ_1 and Φ_2 are 4×4 VAR parameter matrices with elements denoted by $\phi_{ij}^{(1)}$ and $\phi_{ij}^{(2)}$, for $i, j = 1$ (power), 2 (gas), 3 (coal), 4 (carbon), respectively. $\phi_{ij}^{(p)}$ represents the effect of commodity j on commodity i in lag p. Standard errors are reported in parentheses. Superscripts *, **, and *** denote statistical significance at the 10%, 5%, and 1% levels, respectively.

Table 7
Conditional covariance and distributional parameter estimates for the M6/Type6 model.

a_{11}	0.202***	a_{12}	0.017	a_{13}	0.030	a_{14}	0.047
	(0.024)		(0.031)		(0.029)		(0.057)
a_{21}	0.022*	a_{22}	0.244***	a_{23}	0.048***	a_{24}	-0.032
	(0.013)		(0.019)		(0.016)		(0.032)
a_{31}	0.009	a_{32}	-0.001	a_{33}	0.152***	a_{34}	0.003
	(0.012)		(0.012)		(0.016)		(0.029)
a_{41}	0.008**	a_{42}	-0.001	a_{43}	0.004	a_{44}	0.202***
	(0.003)		(0.004)		(0.004)		(0.023)
b_{11}	0.947***	b_{12}	-0.017	b_{13}	-0.015	b_{14}	-0.045*
	(0.009)		(0.012)		(0.011)		(0.024)
b_{21}	0.004	b_{22}	0.971***	b_{23}	-0.012**	b_{24}	0.030
	(0.004)		(0.005)		(0.005)		(0.021)
b_{31}	0.003	b_{32}	0.007*	b_{33}	0.989***	b_{34}	0.008***
	(0.003)		(0.004)		(0.004)		(0.002)
b_{41}	-0.001	b_{42}	0.002	b_{43}	-0.001	b_{44}	0.951***
	(0.001)		(0.001)		(0.001)		(0.005)
c_{11}	-0.052						
	(0.037)						
c_{21}	0.017	c_{22}	0.059***				
	(0.035)		(0.018)				
c_{31}	0.051	c_{32}	0.013	c_{33}	0.041		
	(0.038)		(0.040)		(0.029)		
c_{41}	0.032**	c_{42}	-0.023	c_{43}	0.012	c_{44}	0.246***
	(0.016)		(0.023)		(0.024)		(0.037)
d_{11}	-0.091*	d_{12}	-0.049	d_{13}	-0.025	d_{14}	-0.127
	(0.048)		(0.061)		(0.062)		(0.121)
d_{21}	0.072***	d_{22}	0.004	d_{23}	-0.001	d_{24}	0.078*
	(0.015)		(0.024)		(0.015)		(0.047)
d_{31}	0.102***	d_{32}	0.047	d_{33}	0.104***	d_{34}	0.085***
	(0.025)		(0.035)		(0.038)		(0.023)
d_{41}	-0.002	d_{42}	0.005	d_{43}	0.002	d_{44}	-0.308***
	(0.005)		(0.005)		(0.005)		(0.029)
ξ_1	1.068***	ξ_2	1.130***	ξ_3	0.988***	ξ_4	0.961***
	(0.033)		(0.037)		(0.034)		(0.031)
ν_1^{-1}	0.153***	ν_2^{-1}	0.138***	ν_3^{-1}	0.117***	ν_4^{-1}	0.214***
	(0.015)		(0.024)		(0.024)		(0.026)

Note: The conditional covariance matrix is given in Eq. (3) and specified by the 4×4 matrices A, B, C, and D, the elements of which are denoted by a_{ij}, b_{ij}, c_{ij}, and d_{ij}, for $i, j = 1$ (power), 2 (gas), 3 (coal), 4 (carbon). The C-matrix is lower triangular and, therefore, there are no estimates for the entries above the diagonal. The distributional parameters are reported in the last two rows. Standard errors are reported in parentheses. Superscripts *, **, and *** denote statistical significance at the 10%, 5%, and 1% levels, respectively.

Table 8
Critical quantiles (in percent) in news distribution.

	Positive News			Negative News		
	Gas	Coal	Carbon	Gas	Coal	Carbon
2008	96.93	94.57	99.05	0.33	0.64	1.17
2009	94.91	96.67	99.00	0.50	0.23	1.31
2010	95.05	97.26	99.25	0.63	0.11	1.06
2011	96.84	97.77	98.25	0.39	0.08	2.36
2012	97.80	97.14	98.09	0.16	0.09	2.66
2013	99.58	97.64	96.63	0.01	0.07	4.69
2014	95.91	97.88	98.67	0.31	0.04	2.07
2015	96.36	94.15	99.50	0.25	0.30	0.79

The table shows critical quantiles in the news distribution for different markets. News of a lower magnitude does not lead to a higher than otherwise expected day-ahead variance in the power market.

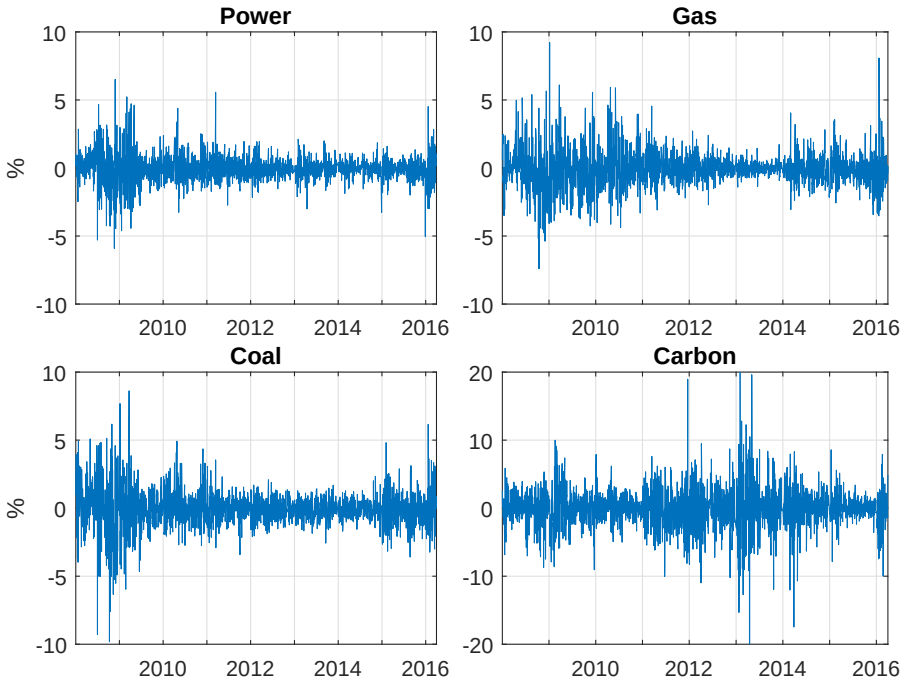

Figure 1: Time series of commodity log-returns.

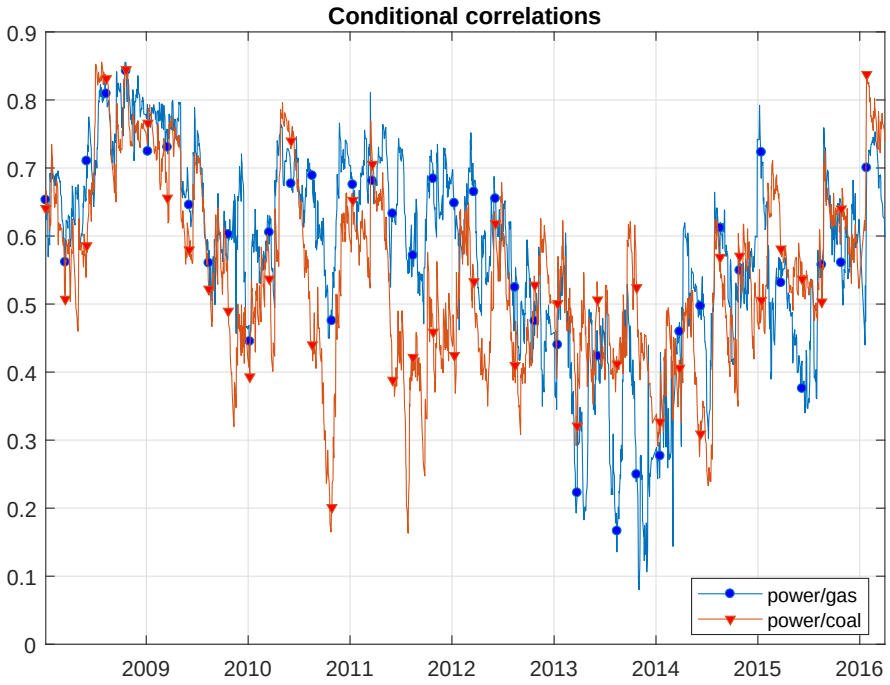

Figure 2: Correlations between power and fuels, as implied by model M6/Type6.

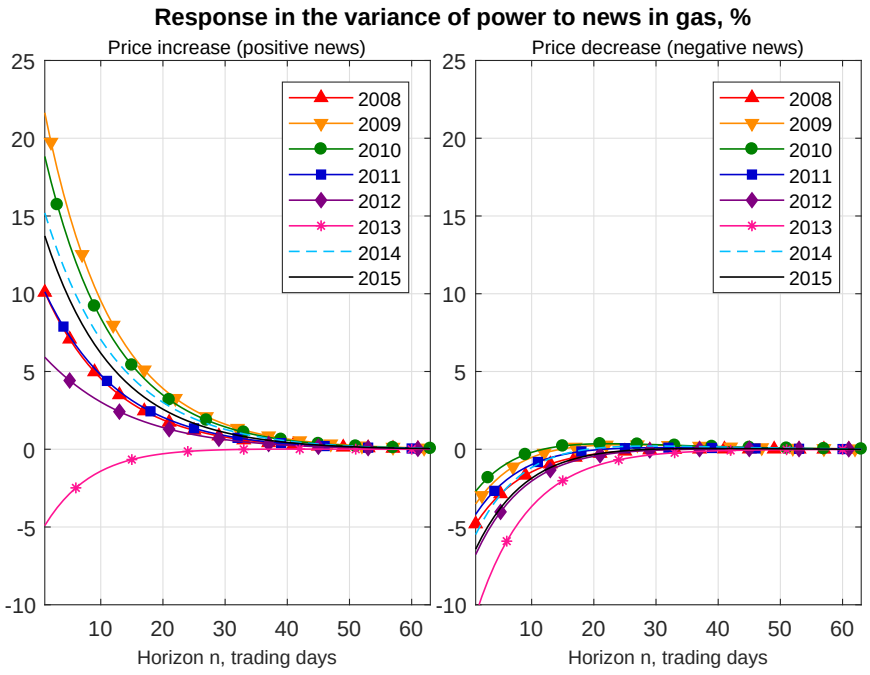

Figure 3: The power VIRF following news in the gas market. The variance responses are plotted against the horizon for each year in 2008–2015, with the horizons ranging from 1 to 63 trading days. The left panel displays responses following gas price increases, while the right panel displays responses following gas price decreases.

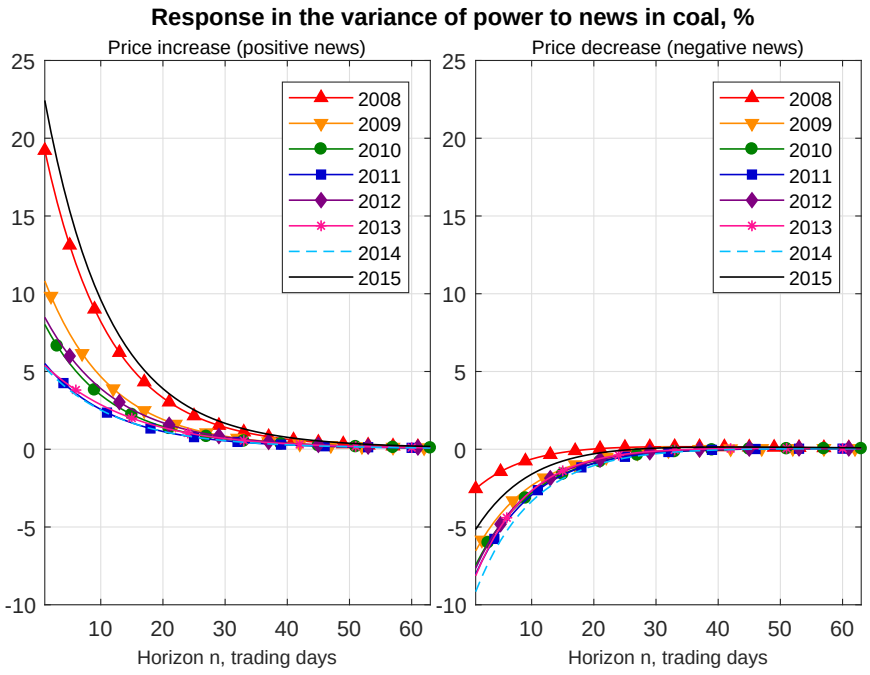

Figure 4: The power VIRF following news in the coal market. The variance responses are plotted against the horizon for each year in 2008–2015, with the horizons ranging from 1 to 63 trading days. The left panel displays responses following coal price increases, while the right panel displays responses following coal price decreases.

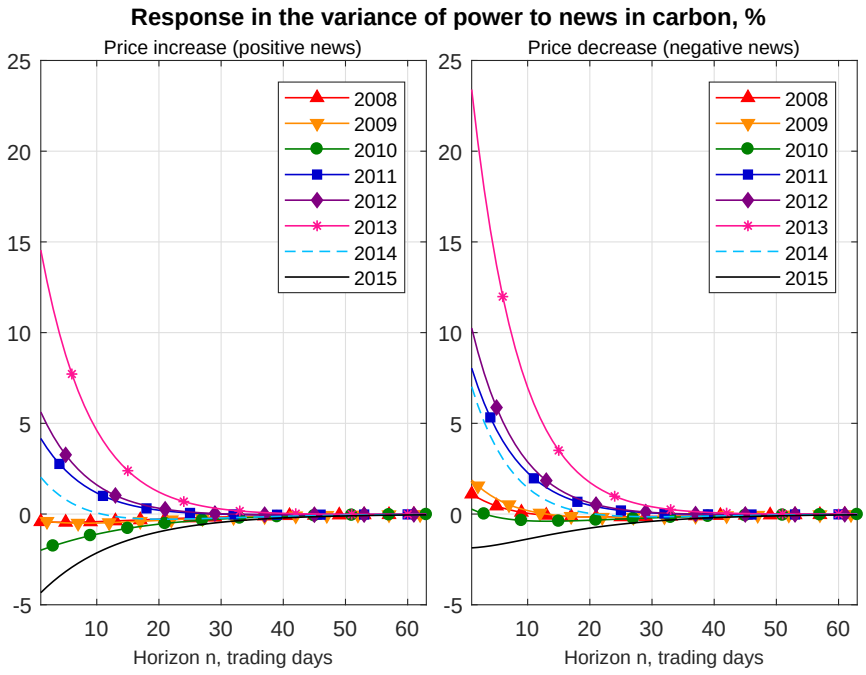

Figure 5: The power VIRF following news in the carbon market. The variance responses are plotted against the horizon for each year in 2008–2015, with the horizons ranging from 1 to 63 trading days. The left panel displays responses following carbon price increases, while the right panel displays responses following carbon price decreases.

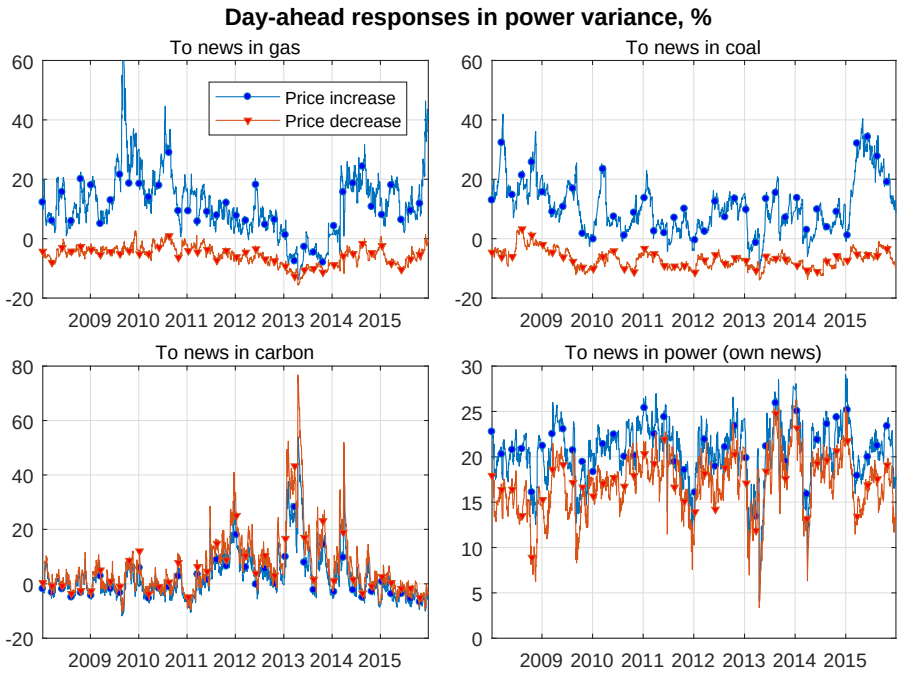

Figure 6: Time series of day-ahead responses in the variance of power. The upper, left panel shows the day-ahead VIRF for power following news in gas; the upper, right panel shows the day-ahead VIRF for power following news in coal; the lower, left panel shows the day-ahead VIRF following news in carbon; and the lower, right panel shows the day-ahead VIRF following news in power (own news).